Philosophical Magazine Letters
Vol. 92, No. 3, March 2012, 111–121

Taylor & Francis
Taylor & Francis Group

Revisiting the intra-granular dislocation extension model for flow stress in nanocrystalline metals

Pei Gu[a]*, Bimal K. Kad[b] and Ming Dao[c]

[a]*MSC Software Corporation, 6050 Scripps St., San Diego, CA 92122, USA;* [b]*Department of Structural Engineering, University of San Diego, San Diego, CA 92122-0085, USA;* [c]*Department of Materials Science and Engineering, Massachusetts Institute of Technology, Cambridge, MA 02139, USA*

(*Received 7 September 2011; final version received 23 October 2011*)

In our previous work (R.J. Asaro, P. Krysl and B. Kad, Philos. Mag. Lett. 83 (2003) p.733; P. Gu, B. Kad and M. Dao, Scr. Mater. 62 (2010) p.361), the intra-granular partial dislocation extension model was shown to be consistent with the experimental data of flow stress in nanocrystalline FCC materials. However, since the averaged extension was taken for a non-uniform loop, the model predicted small dislocation extension across the grain. In this article, extending our previous work, we reformulate the intra-granular partial dislocation model for FCC nanocrystalline materials using a more realistic loop. The flow stress obtained from the reformulated model shows good agreement with experimental data for various nanocrystalline FCC materials and expectedly large dislocation extension across the grain. In the second portion of this article, the mechanistic model for partial dislocation extension is extended to develop an intra-granular perfect dislocation extension model. The perfect dislocation model is examined by comparing its prediction of flow stress with experimental data of nanocrystalline Fe. Additionally, activation volume and strain-rate sensitivity are discussed within the mechanistic model in the light of available experimental data on nanocrystalline Fe.

Keywords: nanograined structures; flow stress; intra-granular dislocation extension

1. Introduction

The grain-size dependent flow stress, as expressed by Hall–Petch relation [1,2], may be interpreted by the dislocation pile-up model [3], the grain-boundary ledge model [4], and the grain-boundary strengthening model [5]. For nano-scaled grains in nanocrystalline FCC materials, Asaro et al. [6] proposed an intra-granular partial dislocation extension model, which envisages the emission of partial dislocations from grain boundaries and recognizes the contribution of two portions of the dislocation loop to flow stress: the portion laid on the side boundary and that extended in the interior of the grain. The flow stress model given in Asaro et al. [6] is a uniform partial dislocation extension model, where the extended portion in the

*Corresponding author. Email: pei.gu@mscsoftware.com

ISSN 0950–0839 print/ISSN 1362–3036 online

http://dx.doi.org/10.1080/09500839.2011.637975
http://www.tandfonline.com

interior is a straight line and parallel to the grain boundary, and which predicts higher flow stress than experimental data. Later, Gu et al. [7] showed that a refined model, called non-uniform partial dislocation extension model which considers the averaged extension distance of the non-uniform loop, is more consistent with the experimental data. However, the extension distance predicted from such averaged treatment of the non-uniform loop is rather small compared to the grain size, see Figures 2 and 3 in reference [7]. Large dislocation extension is possible because dislocation cell structures and large dislocation pileups, which operate in micrograins and which can limit the extension, are not expected in nanograins.

In this article, continuing our previous work [6–9], we take a more realistic non-uniform loop to reformulate the non-uniform partial dislocation extension model for flow stress in searching for the loop shape influence in the nanograins. The prediction of flow stress is consistent with the experimental data and the previous model using averaged treatment of the non-uniform loop for nanocrystalline Ag, Cu, Pd, and Ni; in addition, it expectantly shows larger partial dislocation extension across the grain. In the second portion of this article, the methodology for the partial dislocation model is extended to develop an intra-granular perfect dislocation extension model, which is employed to discuss the deformation mechanism in nanocrystalline BCC structures. A correction factor is introduced to account for the influence of core structure in BCC materials. The prediction is discussed against experimental data of nanocrystalline Fe.

2. Intra-granular dislocation extension model

Consider the dislocation loop shown in Figure 1. A partial dislocation is emitted into the grain from the perfect dislocation that is initially at the grain boundary. The extended loop of the partial dislocation has two portions: intra-granular extending portion inside the grain and the portion laid on the two sides of the grain boundary. Consider the extension marked as 'straight loop' in Figure 1. From references [6] and [7], the shear stress required to extend the distance d^* and to create the stacking fault is $\tau_1 = \Gamma/b - Gb/(12\pi d^*)$, where G is the shear modulus, b the magnitude of Burger's vector, and Γ the stacking fault energy; the shear stress required for creating the side portion is $\tau_2 = Gb/(3d)$. In reference [6], assuming that the partial dislocation is uniformly extended across the entire grain, i.e., the extension distance d^* is taken as the grain size d, above two expressions are combined to obtain the flow stress $\tau = \Gamma/b + G[1/3 - 1/(12\pi)]b/d$. This expression was shown to give higher flow stress than that of experimental data. To correct the overestimation, in reference [7] we took d^* as the averaged extension distance of a non-uniform loop, $d^* = 1/d\int_0^d \delta(x)\,\mathrm{d}x = \beta d$. Then the flow stress from the averaged loop is obtained as $\tau = \Gamma/b + G[1/3 - 1/(12\pi\beta)]b/d$, where $1/(4\pi) \le \beta \le 1$. The minimum for the non-dimensional extension β comes from the requirement that the second term needs to be positive. The β or d^* represents the averaged extension across the grain. With fitted values for the averaged extension parameter, the above flow stress expression, referred as averaged loop model hereafter, matches experimental data, see Figures 2 and 3 in reference [7].

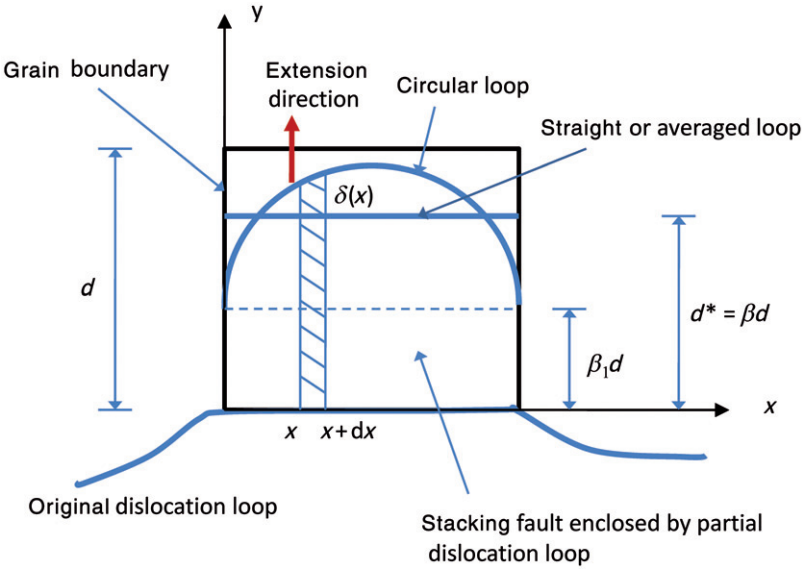

Figure 1. (Color online). Intra-granular dislocation extension model for nanocrystalline materials. For FCC nano-structures, flow stress model is developed by envisioning the emission of partial dislocation into the nanograin. For BCC nano-structures, flow stress model is developed by envisioning the emission of perfect dislocation into the nanograin.

We evaluate flow stress from the partial dislocation extension model using a more realistic intra-granular loop which is marked as 'circular loop' in Figure 1, instead of the averaged loop. Consider the following scenario: when the partial dislocation is emitted into the grain, it is bowed out with its end points of the intra-granular portion pinned at the grain boundary. The radius of the curvature reaches its maximum before the extension is shifted to increase the side segments. Finally, the center of the partial dislocation loop touches the opposite of the grain boundary ($\beta_1 = 0.5$). Another scenario parallel to this is an elliptical-shaped partial dislocation loop which is formed at the early stage of the emission from the grain boundary. Further extension includes the increase of both the radius of curvature for the intra-granular portion and the side segment at the same time. The maximum radius of curvature is attained when the center of the intra-granular portion touches the opposite of the grain boundary ($\beta_1 = 0.5$). From Figure 1, the range of the extension of the side segment is $0 \leq \beta_1 \leq 0.5$. Like before, the shear stress required for such extension consists of two parts: one for the intra-granular portion of the loop and the stacking fault creation and another for the two side segments. The required shear stress for the loop element dx at the position x along the grain boundary to extend distance $\delta(x)$ and create stacking fault, which is bounded by the two vertical lines $y = x$ and $y = x + \mathrm{d}x$, the grain boundary where the dislocation is originally located, and the extended loop, is $\mathrm{d}F/\mathrm{d}x = \{\Gamma/b - Gb/[12\pi\delta(x)]\}$ according to above analysis. Here, $\mathrm{d}F$ is a force per unit length for the loop element dx. Then, the shear stress required for extending the entire intra-granular portion of the loop and creating associated stacking fault is $\tau_1 = 1/d \int_0^d \mathrm{d}F$. Taking the energy per unit length

stored in the side segment as $1/2Gb_1^2$, where b_1 is the magnitude of the partial dislocation's Burgers' vector, from energy balance, we have the shear stress required for extending the side segments, $(\tau_{2x}b_{1x} + \tau_{2y}b_{1y})\int_0^d \delta(x)\mathrm{d}x = Gb_1^2\beta_1 d$. In the expression, b_{1x} and b_{1y} are the components of the partial dislocation along x- and y-axes, respectively; similarly, τ_{2x} and τ_{2y} are the components of the shear stress along x- and y-axes, respectively. Carrying out the above integrations, the shear stress required for the partial dislocation extension is given as follows

$$\tau = \frac{\Gamma}{b} + AG\frac{b}{d}. \tag{1}$$

In Equation (1), the constant is written as

$$A = \frac{\beta_1}{3\left(\frac{\pi}{8} + \beta_1\right)} - \frac{1}{12\pi}\left[\pi - \frac{\beta_1}{\sqrt{\frac{1}{4} - \beta_1^2}}\ln\frac{1 + 2\sqrt{\frac{1}{4} - \beta_1^2}}{1 - 2\sqrt{\frac{1}{4} - \beta_1^2}}\right]. \tag{2}$$

The flow stress in Equation (1), referred as circular loop model hereafter, is in the same form as those in references [6–9], except the multiplier A. In the case of full extension where the center of the loop reaches the opposite of the grain boundary, $\beta_1 = 0.5$, Equation (1) becomes $\tau = \Gamma/b + 0.156\,Gb/d$.

It was shown in reference [7] that the extension β_1 can be chosen such that the intra-granular partial dislocation model is equivalent to the Hall–Petch relation, $\tau = k_0 + k_1/\sqrt{d}$, where k_0 and k_1 are the coefficients of grain-size independent and dependent terms. Here, the grain size is in the range where intra-granular partial dislocation extension operates for strengthening mechanism and therefore $k_1 > 0$. For softening mechanism at very small grain size, where the grain boundary effects are active, see the discussion in the following section. For the circular loop model, if we retain constant term and linear term of β_1 in Equation (2) for estimation, the extension that is equivalent to the Hall–Petch relation is $\beta_1 = 1.129k_1\sqrt{d}/(\mathrm{Gb}) + 0.094$. It is noted here that the extension is proportional to the square root of the grain size, $\beta_1 \sim \sqrt{d}$, such that larger extension can be expected for larger grain size.

Envisioning a perfect dislocation is emitted into the grain, similar approach to the above for the partial dislocation can be applied, and the difference is that in such case no stacking fault is created. For the intra-granular circular loop in Figure 1, the change of loop energy during extension is expressed as $E = (\alpha Gb^2/2)\,\pi d/2 + Gb^2\beta_1 d - (Gb^2/2)d$. Here, α comes from the energy per unit length for the half-circular perfect dislocation loop, $\alpha Gb^2/2$. The α represents the influence of the curved loop and is estimated to be close to 1.0 from the first term of Equation (41) in reference [9] (by letting $\nu = 0$ and $\ln(r/r_0) \approx 2\pi$, where ν is the Poisson's ratio, r_0 the core cut-off radius, and r the loop size). We will discuss this parameter more when examining the perfect dislocation model for BCC structures in Section 4. The change of loop energy is balanced by the work done by shear stress $W = (\pi d^2/8 + \beta_1 d^2)\,\tau b$; this leads to

$$\tau = \frac{2\pi\alpha - 4 + 8\beta_1}{\pi + 8\beta_1}G\frac{b}{d}. \tag{3}$$

The scaling expression in the front of Gb/d in Equation (3) is the property of non-uniform extension. Equation (3) can be viewed as the extension of the traditional line tension model, $\tau = Gb/d$. When $\alpha = (\pi + 4)/(2\pi) = 1.14$, Equation (3) recovers the traditional line tension model.

3. Prediction for FCC metals

At smaller grain size, Equation (1) gives lower value of flow stress compared with that from Equation (3), whereas at larger grain size, the opposite is true. Hence, there is a grain size for the transition from perfect dislocation emission to partial dislocation emission. Asaro and Suresh [9] calculated the transition threshold: 40 nm for Cu; 16 nm for Ni; 84 nm for Ag; and 41 nm for Pd. Here, the threshold for Pd is re-estimated using stacking fault energy 56 mJ/m^2 to be consistent with reference [7]. At very small grain size, of the order ~10 nm or less, instead of the increase of flow stress with respect to the decrease of grain size, flow stress decreases along with grain size [10,11]. This phenomenon is the so-called strength softening. In the circular loop model, it is seen from Equations (1) and (2) that when the extension distance β_1 becomes very small, the coefficient of the grain-size dependent term becomes negative. This is also true for the averaged loop model discussed early, i.e., the coefficient $1/3 - 1/(12\pi\beta)$ becomes negative for very small β. In addition, when the side segments are annihilated through certain reactions at the grain boundary, the first term on the right side of Equation (2) vanishes such that the coefficient of the grain-size dependent term is negative too. Since negative grain-size dependent term implies strength softening, the intra-granular partial dislocation model suggests the transition from strengthening to softening when dislocations around the grain boundary become more active. However, the current model would not be able to quantitatively predict the required shear stress for grain boundary sliding at very small grain size, since it is developed based on the mechanism of intra-granular dislocation extension, not the mechanism of grain boundary sliding. From the thermal activation equation applied to grain boundary sliding, a model relating the required shear stress to shear rate and grain size was proposed by Conrad and Narayan [12] for such strength softening, where the intra-granular partial distortion extension model and perfect dislocation extension model are not applied. The above discussion characterizes the grain size for the intra-granular partial dislocation model.

We plot the flow stress in Equation (1) with full extension, $\beta_1 = 0.5$, in Figure 2a and b against the flow stress from the averaged loop model and experimental data that are recompiled from reference [7] for nanocrystalline Cu and Pd, respectively. The material data for plotting the curves are: for Cu, $G = 50$ GPa, $b = 0.255$ nm, and $\Gamma/(Gb) = 0.00425$; for Pd, $G = 44$ PGa, $b = 0.28$ nm, and $\Gamma/(Gb) = 0.004545$. The grain sizes in the two figures fall into the range where partial dislocation emission is favored. Both plots show that the circular loop model predicts both flow stress that is consistent with the experimental data and sufficiently large dislocation extension distance that can be expected at the onset of plastic deformation. The large extension is because dislocation cell structures and large pileups, which operate in micrograins and which can limit dislocation extension, are not expected to operate in nanograins

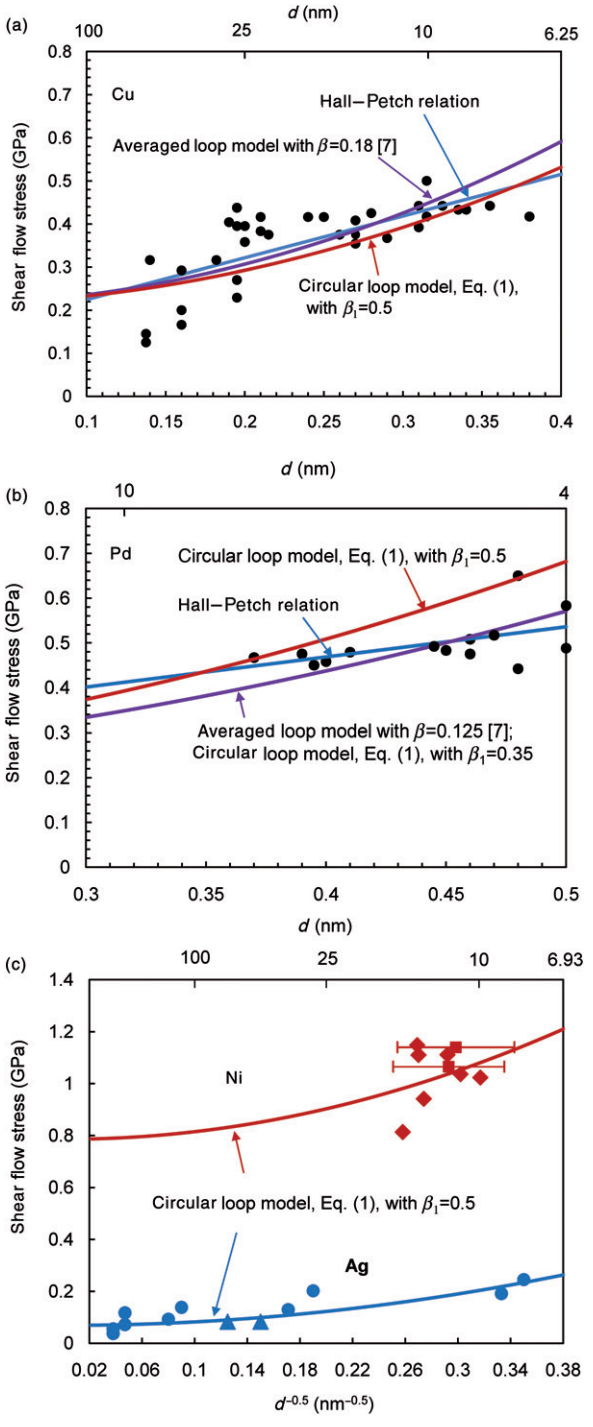

Figure 2. (Color online). Prediction of intra-granular partial dislocation extension model versus experimental data for nanocrystalline FCC metals, (a) Cu; (b) Pd; (c) Ni and Ag. In (c), square symbols from [15]; diamond symbols from [16]; triangle symbols from [17]; circular symbols from [18].

[13,14]. The extension $\beta_1 = 0.5$ corresponds to full extension where the frontier of the circular loop touches the opposite of the grain boundary. As comparison, although the averaged loop model gives consistent flow stress, the extension distance is fairly small portion of the grain size, less than 20% of the grain size ($\beta = 0.18$ and $\beta = 0.125$, respectively). In Figure 2a, the flow stress curve for the circular loop model with full extension fits the data well, whereas in Figure 2b, the flow stress curve for the circular loop model with $\beta_1 = 0.35$ appears to fit the data better than that with the full extension. In Figure 2b, the curve for the circular loop model with $\beta_1 = 0.35$ appears to coincide with that for the averaged loop model with $\beta = 0.125$. Even for $\beta_1 = 0.35$, there is considerably larger extension across the grain.

Figure 2c is a plot of flow stress in Equation (1) with full extension, $\beta_1 = 0.5$, against experimental data for nanocrystalline Ag and Ni. The experimental data are taken from references [15,16] for Ni and [17,18] for Ag. The material data for plotting the curves are: for Ag, $G = 30\,\text{GPa}$, $b = 0.288\,\text{nm}$, and $\Gamma/(Gb) = 0.002285$; for Ni, $G = 76\,\text{PGa}$, $b = 0.248\,\text{nm}$, and $\Gamma/(Gb) = 0.01033$. The experimental data of Ni are at the right side of the figure for grain size less than 16 nm, where the partial dislocation emission is preferred for Ni; and the prediction is consistent with the data. For Ag, the prediction fits the data fairly well. It appears that this good agreement even extends to the very left of the figure beyond the upper bound of the range predicted for the partial dislocation emission in Ag. Among the four nanocrystalline materials, the ranking of the prediction from Equation (1), beginning with the best, is Ag, Cu, Pd, and Ni. This fact may be understood from the following perspective. For Ag, which has the lowest stacking fault energy among the four, intra-granular partial dislocation extension is relatively easier to overcome the energy barrier of the stacking fault and therefore is likely a dominant deformation mechanism. For the materials with higher stacking fault energy, e.g., Ni, the higher required shear stress to overcome the energy barrier to create the stacking fault may also simultaneously induce grain boundary sliding. In reference [8], both intra-granular partial dislocation extension and grain boundary sliding were considered for a nanograin in the formulation of a 3D viscoplastic, rate-dependent constitutive relationship for studying the influence of grain-size distribution in nano-enhanced polycrystalline aggregates. For nanocrystalline FCC structures, the other two major parameters that characterize plastic deformation, activation volume and strain-rate sensitivity, were discussed within the mechanistic model in references [9] and [19].

4. Prediction for BCC metals

In this section, we examine the intra-granular perfect dislocation model, developed in Section 2, for nanocrystalline BCC structure's flow stress by comparing its prediction with available experimental data. For BCC structures, there has been no direct experimental evidence of stable stacking fault [20]. Atomistic scaled simulations suggest that stacking fault created by an assumed partial dislocation in the hard ball model, where atoms are in the depressed positions in a crystallographic plane, is unstable [21,22], i.e., the generalized stacking fault energy does not achieve the minimum with respect to the atoms' positions. This fact suggests that stable intrinsic stacking fault does not likely exist in BCC structures. Therefore, we use the

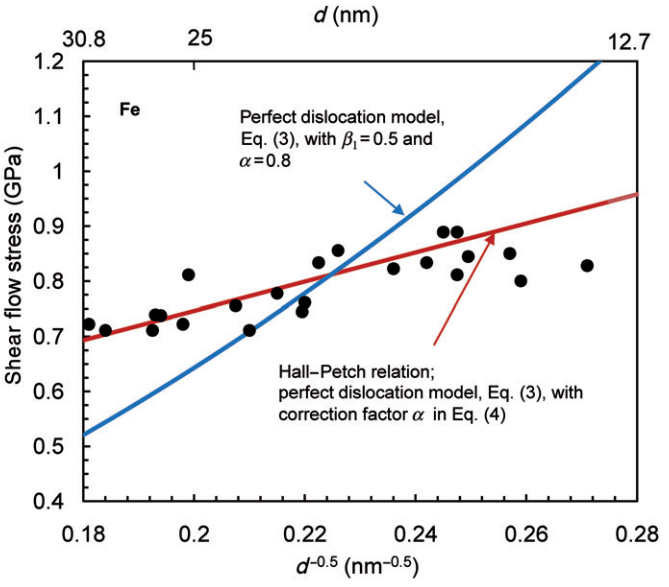

Figure 3. (Color online). Prediction of intra-granular perfect dislocation extension model versus experimental data for nanocrystalline Fe.

intra-granular perfect dislocation model, Equation (3), for BCC structures. Figure 3 is a plot of predicted flow stress from Equation (3) and experimental data, along with the fitted curve from Hall–Petch relation, for nanocrystalline Fe. The experimental data are taken from reference [23], and the prediction is obtained using $G = 82$ GPa, $b = 0.28$ nm, $\alpha = 0.8$ and $\beta_1 = 0.5$. The prediction is not in satisfactory agreement with the data, although it is in the same order of magnitude as the data.

The unsatisfactory agreement may reflect the unique nature of BCCs in plastic deformation: the non-planar character of core structure and asymmetric character with respect to external loading [20–22]. The change in the *discrete* core structure was unable to be considered in the intra-granular perfect dislocation model, Equation (3), from dislocation theory. Taking α as a constant that is independent of grain size was an estimate from the energy of a half-circular loop without considering the nature of Burgers vector. We redefine α in Equation (3), and let it also account for the influence of these unique characters in BCCs, in addition to the influence of the curved loop in dislocation theory. In other words, the correction leads to a better representation for the loop energy to include those effects which may not be neglected in BCC's deformation and which were not accounted for in the energy evaluation from dislocation theory. The modified parameter α may be determined by fitting experimental data. Let the fitting of Hall–Petch relationship to the data in Figure 3 be equal to the flow stress in Equation (3). This gives

$$\alpha = \frac{\pi + 4}{2\pi G} \frac{d}{b} \left(k_0 + k_1 \frac{1}{\sqrt{d}} \right). \tag{4}$$

Table 1. Correction factor for the energy of dislocation loop in nanocrystalline Fe.

d (nm)	15	20	25	30
α	0.67	0.80	0.92	1.04

The condition for Equation (4) is that the grain size is in the range where intra-granular dislocation extension operates for strengthening mechanism such that $k_1 > 0$. Equation (4) not only recasts the intra-granular perfect dislocation extension model to be equivalent to Hall–Petch relation but also links it to the experimental data through the fitted Hall–Petch coefficients k_0 and k_1. Using the fitted coefficients of Hall–Petch relation, several values of α obtained from Equation (4) are listed in Table 1, and these values are consistent with the estimation from dislocation theory in Section 2. In the table, it appears that the larger the grain size, the larger the parameter. Examining Equation (3) against reported flow stress data for other nanocrystalline BCC metals, such as Ta and Mo [24], also suggests the correction to α. When the correction factor α may not be accurately obtained from dislocation theory, Equation (4) provides a means to evaluate it from the Hall–Petch type fitting of experimental data. Equation (4) also suggests that α is grain-size dependent.

The activation volume V of nanocrystalline Fe, evaluated from the energy approach that envisions dislocation loop initiation from a crack-like stress concentration source [9], is $12b^3$, which is consistent with the activation volume obtained from another approach discussed in reference [19] in the order of the magnitude. The strain-rate sensitivity may be evaluated from its definition [9], $m = \sqrt{3}kT/(V\sigma)$, where σ is tensile flow stress. A representative value of flow stress in Figure 3 and the above expression for activation volume are used to estimate the order of magnitude for strain-rate sensitivity. If choosing $\sigma = 3\tau = 2.4\,\text{GPa}$ and $b = 0.28\,\text{nm}$, we obtain $m \approx 0.01$. The order of magnitude is consistent with those reported in references [25,26]. The variation of strain-rate sensitivity with respect to grain size for BCC materials was qualitatively discussed within dislocation theory in reference [27]. However, there are limited data for grain size below 100 nm to further characterize the size-dependent strain-rate sensitivity at the nanoregion.

5. Summary

In summary, the intra-granular partial dislocation extension model is reformulated using a more realistic non-uniform loop for nanocrystalline FCC structures. The predictions for flow stress show good agreement with experimental data of nanocrystalline Ag, Cu, Pd, and Ni. In addition, the model shows sufficiently large extension across the grain, compared with the previous averaged loop model. It is noted that the envision of emitting intra-granular partial dislocations, which was used to develop the partial dislocation extension model, was also employed to model deformation twinning in nanocrystalline FCC materials [28,29]. For nano-twins in

ultra-fine grains synthesized using pulsed electrodeposition [30], it is seen in references [19,31–34] that intra-twin slip and inter-twin slip play an important role in strengthening. In the second portion of this article, as a preliminary investigation of the intra-granular perfect dislocation extension model for nanocrystalline BCC metals, the prediction for flow stress of nanocrystalline Fe is compared with experimental data, and a correction factor is introduced to account for the influence of core structure in BCC materials. The obtained data for the correction factor indicates its grain-size dependence; this suggests that the influence of the loop curvature or the change of core structure may be related to grain size. Activation volume and strain-rate sensitivity are also discussed in the context of available experimental data of nanocrystalline Fe.

For nanocrystalline FCC metals, the fact that the averaged loop model and the circular loop model give similar flow stresses but difference extension distances, Figure 2a and b, suggests non-uniqueness: various intra-granular dislocation loops can exist during plastic deformation of a nanocrystalline material even with uniform grain size. The non-uniqueness of dislocation loops within dislocation theory was noted in reference [7]: an averaged loop represents various possible dislocation loops. This non-uniqueness is further illustrated here since despite of significant differences in extension distances in Figure 2a and b (i.e., significant different values of β and β_1), similar flow stresses are achieved. This again suggests that flow stress in a FCC nano-material to characterize its plastic deformation can be modeled by envisioning the non-uniform partial dislocation extension within dislocation theory, but accurately describing real-time dislocation extension appears to be beyond the dislocation theory and requires atomistic scaled simulations discussed in references [35–38].

Acknowledgments

MD acknowledges the financial support by the ONR Grant N00014-08-1-0510 and by the Advanced Materials for Micro and Nano Systems Programme of the Singapore-MIT Alliance (SMA).

References

[1] E.O. Hall, Proc. Phys. Soc. London B64 (1951) p.747.
[2] N.J. Petch, J. Iron Steel Res. Int. 174 (1953) p.25.
[3] A.H. Cottrell, Trans. Metall. Soc. AIME 212 (1958) p.192.
[4] J.C.M. Li, Trans. Metall. Soc. AIME 227 (1963) p.239.
[5] M.A. Meyers and E. Ashworth, Philos. Mag. A46 (1982) p.737.
[6] R.J. Asaro, P. Krysl and B. Kad, Philos. Mag. Lett. 83 (2003) p.733.
[7] P. Gu, B. Kad and M. Dao, Scr. Mater. 62 (2010) p.361.
[8] B. Zhu, R.J. Asaro, P. Krysl and R. Bailey, Acta Mater. 53 (2005) p.4825.
[9] R.J. Asaro and S. Suresh, Acta Mater. 53 (2005) p.3369.
[10] A.H. Chokshi, A. Rosen, J. Karch and H. Gleiter, Scr. Mater. 23 (1989) p.1679.
[11] K. Lu and M.L. Sui, Scr. Mater. 28 (1993) p.1465.
[12] H. Conrad and J. Narayan, Scr. Mater. 42 (2000) p.1025.
[13] H. Conrad, Metall. Mater. Trans. 35A (2004) p.2681.

[14] M.A. Meyers, A. Mishra and D.J. Benson, Prog. Mater. Sci. 51 (2006) p.427.
[15] G.D. Hughes, S.D. Smith, C.S. Pande, H.R. Johnson and R.W. Armstrong, Scr. Mater. 20 (1986) p.93.
[16] A.F. Zimmerman, G. Palumbo, K.T. Aust and U. Erb, Mater. Sci. Eng. A328 (2002) p.137.
[17] G.W. Nieman, J.R. Weertman and R.W. Siegel, Nanostruct. Mater. 1 (1992) p.185.
[18] T. Kizuka, H. Ichinose and Y. Ishida, J. Mater. Sci. 32 (1997) p.1501.
[19] P. Gu, M. Dao, R.J. Asaro and S. Suresh, Acta Mater. 59 (2011) p.6861.
[20] D. Hall and D.J. Bacon, *Introduction to Dislocations*, Butterworth-Heinemann, Oxford, 2007.
[21] V. Vitek, Crystal Lattice Defects 5 (1974) p.1.
[22] M.S. Duesbery and V. Vitek, Acta Mater. 46 (1998) p.1481.
[23] T.R. Malow and C.C. Koch, Metall. Mater. Trans. 29A (1998) p.2285.
[24] M. Zhang, B. Yang, J. Chu and T.G. Nieh, Scr. Mater. 54 (2006) p.1227.
[25] D. Jang and M. Atzmon, J. Appl. Phys. 93 (2003) p.9282.
[26] T.R. Malow, C.C. Koch, P.Q. Miraglia and K.L. Murty, Mater. Sci. Eng. A252 (1998) p.36.
[27] Q. Wei, S. Cheng, K.T. Ramesh and E. Ma, Mater. Sci. Eng. A381 (2004) p.71.
[28] Y.T. Zhu, X.Z. Liao, S.G. Srinivasan, Y.H. Zhao, M.I. Baskes, F. Zhou and E.J. Lavernia, Appl. Phys. Lett. 85 (2004) p.5049.
[29] Y.T. Zhu, X.Z. Liao and X.L. Wu, Prog. Mater. Sci. 57 (2012) p.1.
[30] L. Lu, R. Schwaiger, Z.W. Shan, M. Dao, K. Lu and S. Suresh, Acta Mater. 53 (2005) p.2169.
[31] Y. Kulkarni and R.J. Asaro, Acta Mater. 57 (2009) p.4835.
[32] M. Dao, L. Lu, Y.F. Shen and S. Suresh, Acta Mater. 54 (2006) p.5421.
[33] A. Jerusalem, M. Dao, S. Suresh and R. Radovitzky, Acta Mater. 56 (2008) p.4647.
[34] L. Lu, M. Dao, T. Zhu and J. Li, Scr. Mater. 60 (2009) p.1062.
[35] H. Van Swygenhoven, M. Spaczer and A. Caro, Acta Mater. 47 (1999) p.3117.
[36] T. Zhu, J. Li, A. Samanta, H.G. Kim and S. Suresh, PNAS 104 (2007) p.3031.
[37] X. Li, Y. Wei, L. Lu, K. Lu and H. Gao, Nature 464 (2010) p.877.
[38] M.P. Dewald and W.A. Curtin, Philos. Mag. 87 (2007) p.4615.